# Glass transition in a simple stochastic model with back-reaction

František Slanina*
*Institute of Physics, Academy of Sciences of the Czech Republic, Na Slovance 2, CZ-18221 Praha, Czech Republic*

Petr Chvosta†
*Department of Macromolecular Physics, Faculty of Mathematics and Physics, Charles University, V Holešovičkách 2, CZ-180 00 Praha, Czech Republic*

(Received 21 August 2003; revised manuscript received 19 December 2003; published 15 April 2004)

We formulate and solve a model of dynamical arrest in colloids. A particle is coupled to the bath of statistically identical particles. The dynamics is described by Langevin equation with stochastic external force described by telegraphic noise. The interaction with the bath is taken into account self-consistently through the back-reaction mechanism. Dynamically induced glass transition occurs for certain value of the coupling strength. Edwards-Anderson parameter jumps discontinuously at the transition. Another order parameter can be also defined, which vanishes continuously with exponent $1/2$ at the critical point. Nonlinear response to harmonic perturbation is found.

DOI: 10.1103/PhysRevE.69.041502 PACS number(s): 64.70.Pf, 02.50.Ey, 05.40.−a

## I. INTRODUCTION

Glass transition and slow relaxation in systems characterized by weak ergodicity breaking remains still an open area, despite many efforts and numerous significant results in the last decade [1–22]. Among the host of diverse phenomena we are motivated here mostly by the effect of dynamical arrest in colloidal matter [23–31], observed experimentally and thoroughly investigated by numerical simulations and mode-coupling method. Below the transition point, the dynamics effectively leads to a glassy state with diverging viscosity, however, the static thermodynamic transition may not be identifiable. Indeed, dynamical or structural arrest demonstrates the glass transition as a purely dynamic and self-consistent phenomenon, where casual slow down of certain particles prevents some other particles from moving, which may slow down the others even more, etc. The self-consistent nature of the phenomenon is reflected by the analytical approaches available now. One of the most striking phenomena in colloids, suspensions, and granular matter is the non-Newtonian response to mechanical perturbation. On one hand, we can have shear thinning, which amounts to a decrease if viscosity due to applied field, which can be interpreted as restoration of ergodicity due to perturbation [25]. On the other hand, increase of viscosity may result in shear thickening or even jamming, typically observed in particulate or granular matter [32,33].

From the theoretical side, the mode-coupling (MC) equations provide us with a well-established framework, capable of explaining a good deal of experimental data [34–37]. The attempts to derive the MC equations starting from the Hamiltonian of the system were successful in the mean-field approximation. It was perhaps the *p*-spin spherical model [4–6,13], where the machinery reached the farther edge of our current understanding of the phenomenon.

However, the bottom-up approach starting with writing explicit Hamiltonians is far from being complete. The presence of the parametrization invariance [13,38] leaves the numerical solution of the MC equations as the only means for obtaining the true time dependence of the correlation and response functions. Also the mean-field approximation generally used now seems to be very difficult to overcome.

The serious difficulties remaining in using the more advanced MC techniques leave the space for more simple phenomenological approaches. We want to follow this path in the present work.

Indeed, the mathematical substance of the mode-coupling method can be summarized by saying that the time dependence of the correlation (and response) functions depends nonlinearly and in time-delayed manner on these functions themselves. Actually, the memory kernel in the MC equations, which is primarily dictated by the properties of the reservoir, depends on the system dynamics.

We may represent the dynamics of the system by a stochastic process and the parameters of the process depend on time through the averaged properties of the process itself. In order to study generic properties of such problems it can be useful to establish a simple idealized model, which would capture the essential mathematic ingredients while avoiding the complications which arise from choosing a specific Hamiltonian at the beginning. The most important ingredient in such an idealized model should be the mechanism of the *back-reaction*.

We introduced recently [39] a very simple stochastic process, in which the back-reaction leads to rich dynamic behavior. The main characteristics was the presence of a phase transition from ergodic to nonergodic phase. The principal aim of the present work is to investigate analytically some of the properties of the transition and from the numerical solution of the corresponding differential equations infer the nontrivial critical behavior.

*Electronic address: slanina@fzu.cz
†Electronic address: chvosta@kmf.troja.mff.cuni.cz

 

## II. LANGEVIN EQUATION WITH BACK–REACTION

### A. System of coupled particles

The model system we will have in mind will be composed of particles, relaxing to their equilibrium positions under the influence of surrounding particles. They can be viewed as colloidal particles immersed in a solvent, but the formulation of our model is generic enough to allow for other interpretations as well, e.g., they can be viewed as microdomains in a relaxor ferroelectric material.

The time evolution of the model can lead to dynamical arrest, where particles are locked in their positions by surrounding particles, which are also locked in their turn. Therefore, the dynamics can lead to the spatially disordered but time-stable stationary state with glass properties. The indication of the glass transition will be the nonzero value of the Edwards-Anderson order parameter and sensitivity to initial conditions. The interaction between particles will be taken into account on a phenomenological level; if we concentrate on a randomly selected particle (single relaxor), the external field from the rest of the system (reservoir) will change as the states of the other particles (relaxors in reservoir) evolve. The changes in the local external field will be the more rapid the faster is the evolution of the other particles. This leads to the idea of expressing the intensity of the changes in the external field through the velocity of movement of the relaxors in the reservoir. As we suppose all particles to be statistically identical, the movement of our single relaxor should be in probabilistic sense equivalent to the movement of any relaxor within the reservoir. This consideration closes the loop.

We will try to express the intensity of the changes of the local field through the averaged properties of the movement of the single relaxor itself. This introduces the idea of *back-reaction:* the probabilistic properties of the reservoir dictate the system evolution and the averaged system dynamics tunes the properties of the reservoir itself.

To be more specific, our single relaxor will be described by the continuous real stochastic variable $\mathsf{X}(t)$. It will evolve under influence of the environmental force, represented by the stochastic variable $\mathsf{Q}(t)$. The force will be modeled by a two-valued random process $\mathsf{Q}(t) \in \{-q, +q\}$ [40], jumping at random instants. Occurrence of the jumps are governed by a self-exciting point process [41,42] with time-dependent intensity $\frac{1}{2}\lambda(t)$.

For given (friction-reduced) force $\mathrm{Q}(t)$ the single relaxor is described by the Langevin equation [44–46]

$$\frac{d}{dt}\mathsf{X}(t) = -\gamma\,\mathsf{X}(t) + \mathsf{Q}(t) \tag{1}$$

with initial conditions $\mathsf{X}(0)=\mathsf{X}_0$ and $\mathsf{Q}(0)=\mathsf{Q}_0$.

We may consider the process $\mathsf{X}(t)$ as a movement of an overdamped particle which slides in a parabolic potential well; the parabola jumps between two positions at random instants, with time-dependent rate $\frac{1}{2}\lambda(t)$.

In reality, of course, we should take into account also the inertial term with second time derivative of the coordinate. This term is neglected here taking implicitly the limit of damping going to infinity while keeping the force to damping ratio finite. We expect the usual damped regime be recovered for the oscillations around the equilibrium positions of the frozen particles. The vibrational states superimpose over the relaxational behavior described mainly in this paper. We believe it does not interfere substantially with the freezing dynamics studied here and therefore the two phenomena can be treated separately. However, this goes beyond the aim of our work. For recent results on vibrational properties of glassy systems see, e.g., Ref. [43].

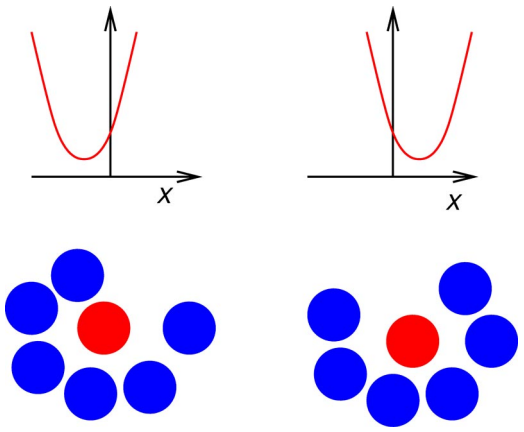


FIG. 1. (Color online) Schematic picture of the particle moving within a cage which can assume two discrete configurations. The cage is represented by a parabolic potential which can be centered around two possible equilibrium positions.

The choice of bimodal environmental force is motivated by the following consideration. The dynamics of a glassy system is dominated by the cage effect, where any chosen particle feels itself trapped within a configuration of surrounding particles forming a cage.

The system has two separate time scales, the shorter one describing the relaxation of the particle within the cage, the longer one corresponding to changes in the cage configuration. We therefore assume that the cage, when excited, finds quickly its equilibrium configuration and remains there for a relatively longer time until it is excited again. Moreover, we suppose the cage can assume discrete set of configurations, such as those sketched schematically in Fig. 1. For the sake of simplicity we reduce this set of cage configurations to two.

The jumps from one to the other configuration occur at the shorter time scale and for the *cage* dynamics we approximately consider this fast dynamics as instantaneous. Therefore, we arrive at the description of the cage dynamics as a sequence of instantaneous jumps between two possible states. The frequency of the jumps $\frac{1}{2}\lambda(t)$ determines the longer time scale.

On the other hand, the fast and slow processes should be coupled somehow, as they are two manifestations of the same dynamic process. Here this coupling will be implemented by the mechanism we call back-reaction.

The intensity of the process, or the frequency of jumps, $\frac{1}{2}\lambda(t)$, is related to the movement of the surrounding relaxors, considered as a reservoir. Intuitively the frequency must be smaller if the movement of the relaxors is slower. Therefore,

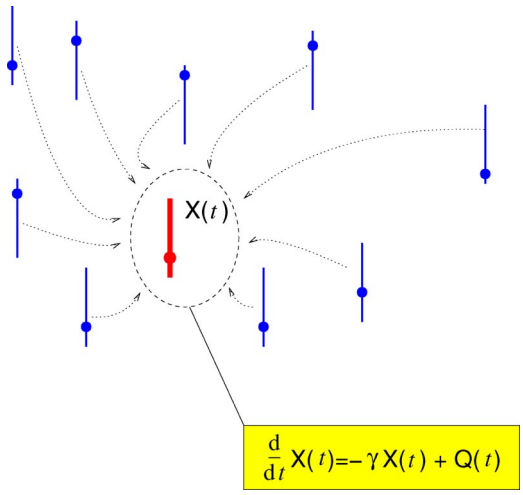


FIG. 2. (Color online) Schematical picture of our model. Relaxing particles in the reservoir influence the relaxation of the selected particle, described by the Langevin equation shown in the frame box.

the function $\lambda(t)$ should be coupled to the velocity $V(t) = (d/dt)\, X(t)$.

However, it is not obvious *a priori* what should be the specific functional dependence. We only require that the dependence is described by a non-negative function analytic at the origin. The simplest choice satisfying this property is

$$\lambda(t) = \epsilon \frac{\gamma}{q^2} \langle V^2(t) \rangle, \tag{2}$$

where $\epsilon$ is the dimensionless coupling strength parameter. The latter prescription is the form of the back-reaction we will study in the following. The model described above is sketched schematically in Fig. 2.

The parameters $\gamma$ and $q$ can be in principle rescaled to 1 by appropriate choice of the units of time and length. Therefore, the coupling strength $\epsilon$ remains to be the only physically relevant parameter tuning the behavior of the system. As we will see, there is a qualitative change in the behavior of the system at a certain critical value of $\epsilon$.

The physical meaning of the parameters $\gamma$ and $\epsilon$ can be formulated as follows. The parameter $\gamma$ arises as a limit of the fraction of spring constant and damping. As the damping is essentially proportional to temperature, the parameter $\gamma$ is related to inverse temperature. This observation can be put on a more firm basis using the fluctuation-dissipation theorem, where the response and correlation functions are related through a constant which is inverse temperature. We will return back to this point in Sec. VI when we will discuss the response of the system to external perturbation.

The interpretation of $\epsilon$ is less straightforward. As mentioned earlier, it quantifies the back-reaction mechanism which relates the long- and short-time processes. Therefore $\epsilon$, or rather the combination $\epsilon\gamma/q^2$ occurring in Eq. (2), relates the cage dynamics to the individual particle dynamics. We expect, e.g., that for higher density of particles the movement of a single particle will be less likely to change the cage configuration, while with lower density the shape of the cage will follow more closely the movement of an individual particle. In such situation $\epsilon$ would decrease with increasing density.

However, both in the relation (2) and in the fluctuation-dissipation relation which we will investigate in Sec. VI the parameters $\epsilon$ and $\gamma$ occur in combination.

The back-reaction mechanism specified in Eq. (2) is the main ingredient which induces the freezing transition in our model. It corresponds to expressing the memory kernel in MC equations by the correlation functions which themselves are to be computed. Both in more sophisticated MC theory and our simple approach the essential meaning is to provide relationship between the dynamics of a particle within a cage and the dynamics of the cage itself. As the glass transition is found in MC theories with diverse forms of the kernel, we expect also here the transition occurring for various functional forms of the back-reaction. Thus, the choice (2) is a simple representative of a whole class of similar back-reaction schemes. On the other hand, surely there are functional forms, which are not powerful enough to yield the transition. We expect the criterion being related to the value of the power, with which the velocity V(t) appears in a formula such as our Eq. (2).

### B. Properties of the environmental force Q(*t*)

The force $Q(t)$ is a time-inhomogeneous Markov process, therefore its properties are fully described by a master equation. More specifically, let us define the probabilities

$$\pi_{\pm}(t) = \mathrm{Prob}\{\, Q(t) = \pm q\} \tag{3}$$

making the vector $\boldsymbol{\pi}(t) = \begin{pmatrix} \pi_-(t) \\ \pi_+(t) \end{pmatrix}$, which satisfies the Pauli master equation

$$\frac{d}{dt}\boldsymbol{\pi}(t) = -\frac{1}{2}\lambda(t)\begin{pmatrix} 1 & -1 \\ -1 & 1 \end{pmatrix}\boldsymbol{\pi}(t). \tag{4}$$

Solving the equation amounts to calculation of the corresponding time-ordered exponential. The averages and correlation functions can be expressed through the integrated intensity

$$\Lambda(t) = \int_0^t \lambda(t')dt'. \tag{5}$$

The time dependence of the vector $\boldsymbol{\pi}(t)$ can be written through the semigroup operator

$$R(t,t_0) = \begin{pmatrix} 1 & 0 \\ 0 & 1 \end{pmatrix} + \frac{1}{2}(e^{-\Lambda(t)+\Lambda(t_0)} - 1)\begin{pmatrix} 1 & -1 \\ -1 & 1 \end{pmatrix} \tag{6}$$

as $\boldsymbol{\pi}(t) = R(t,t_0)\boldsymbol{\pi}(t_0)$. Note that the semigroup operator obeys $R(t,\tau)R(\tau,t_0) = R(t,t_0)\,\forall\,\tau \in [t_0,t]$, which testifies the Markov property of the process.

More explicitly, we find

$$\langle Q(t) \rangle = \langle Q_0 \rangle \exp[-\Lambda(t)], \tag{7}$$

$$\langle \mathsf{Q}(t)\mathsf{Q}(t_1)\rangle = q^2 \exp[-|\Lambda(t)-\Lambda(t_1)|]. \tag{8}$$

Similarly, also the higher correlation functions can be written as products of exponentials with combinations of $\Lambda(t)$ with appropriate time arguments in the exponents. In fact, higher order correlation functions factorize into product of first- and second-order correlations, e.g.,

$$\left\langle \prod_{l=1}^{2k} \mathsf{Q}(t_l) \right\rangle = \prod_{l=1}^{k} \langle \mathsf{Q}(t_{2l})\mathsf{Q}(t_{2l-1})\rangle \tag{9}$$

for $t_{2k} \geqslant t_{2k-1} \geqslant \cdots \geqslant t_2 \geqslant t_1$. Another consequence is that the cumulants of order higher than two vanish.

Note that the function $\Lambda(t)$ is nondecreasing and can either diverge [if $\lim_{t\to\infty}\lambda(t)>0$] or assume a finite limit for $t\to\infty$, if $\lambda(t)$ approaches 0 fast enough.

## III. GLASS TRANSITION AND ASYMPTOTIC RELAXATION

### A. Equations for moments

For any given realization of the process $\mathsf{Q}(t)$, the formal solution of Eq. (1) is

$$\mathsf{X}(t) = \mathsf{X}_0\, e^{-\gamma t} + \int_0^t e^{-\gamma(t-t')}\mathsf{Q}(t')dt'. \tag{10}$$

If the function $\lambda(t)$ were known, various moments (and correlation functions) of the random process $\mathsf{X}(t)$ could have been computed from Eq. (10) using the expressions (7) and (8). However, in our case the function $\lambda(t)$ should be computed from the condition (2), relating it to the second moment of the time derivative of $\mathsf{X}(t)$. This suggests that sufficiently broad set of moments of $\mathsf{X}(t)$ and $\mathsf{V}(t)$ may provide a closed set of ordinary differential equations. The solution of this set will yield the closed description of the behavior of our model.

Indeed, we can define four auxiliary functions

$$s_1(t) = e^{-\Lambda(t)}, \tag{11}$$

$$s_2(t) = e^{-\gamma t}\int_0^t dt'\; e^{\gamma t' - \Lambda(t')}, \tag{12}$$

$$s_3(t) = e^{-\gamma t - \Lambda(t)}\int_0^t dt'\; e^{\gamma t' + \Lambda(t')}, \tag{13}$$

$$s_4(t) = e^{-2\gamma t}\int_0^t dt'\; e^{\gamma t' - \Lambda(t')}\int_0^{t'} dt''\; e^{\gamma t'' + \Lambda(t'')}, \tag{14}$$

and express the requested quantities through these functions. For example, the average coordinate can be written as

$$\langle \mathsf{X}(t)\rangle = \langle \mathsf{X}_0\rangle\, e^{-\gamma t} + \langle \mathsf{Q}_0\rangle\, s_2(t). \tag{15}$$

Similarly, the second moment of the coordinate is

$$\langle \mathsf{X}^2(t)\rangle = \langle \mathsf{X}_0^2\rangle\, e^{-2\gamma t} + 2\langle \mathsf{X}_0\mathsf{Q}_0\rangle\, e^{-\gamma t}\, s_2(t) + 2q^2\, s_4(t). \tag{16}$$

The functions $s_1(t)$ to $s_4(t)$ can be found by solving the set of nonlinear differential equations

$$\dot{s}_1(t) = -\lambda(t)s_1(t), \tag{17}$$

$$\dot{s}_2(t) = -\gamma\, s_2(t) + s_1(t), \tag{18}$$

$$\dot{s}_3(t) = 1 - [\gamma + \lambda(t)]\, s_3(t), \tag{19}$$

$$\dot{s}_4(t) = -2\gamma\, s_4(t) + s_3(t), \tag{20}$$

with initial conditions $s_1(0)=1$, $s_2(0)=s_3(0)=s_4(0)=0$. The function $\lambda(t)$ occurring in the latter equations is itself a combination of the functions $s_1(t)$ to $s_4(t)$:

$$\lambda(t) = \epsilon[\gamma - 2\gamma^2\, s_3(t) + 2\gamma^3\, s_4(t)] + \frac{\epsilon\gamma^2}{q^2}[\gamma\langle \mathsf{X}_0^2\rangle\, e^{-2\gamma t} + 2\gamma\langle \mathsf{X}_0\mathsf{Q}_0\rangle\, e^{-\gamma t}\, s_2(t) - 2\langle \mathsf{X}_0\mathsf{Q}_0\rangle e^{-\gamma t}\, s_1(t)]. \tag{21}$$

In the following we will assume that the initial condition of the stochastic process is $\mathsf{X}_0=0$ and $\langle \mathsf{Q}_0\rangle=0$, except explicitly mentioned cases. This leads to significant simplification of the mathematical structure of the equations. Indeed, the equations for $s_3(t)$ and $s_4(t)$ form a closed pair of equations

$$\dot{s}_3(t) = 1 - (1+\epsilon)\gamma\, s_3(t) + 2\epsilon\gamma^2\,[s_3(t) - \gamma\, s_4(t)]\, s_3(t),$$

$$\dot{s}_4(t) = s_3(t) - 2\gamma\, s_4(t). \tag{22}$$

Unfortunately, the system (22) cannot be solved analytically. The best one can do is to transform the nonlinear Ricatti-type set (22) to one differential equation of Abel type, whose solution, however, is not generally known. Therefore, we will solve Eqs. (22) numerically. Nevertheless, there is still a significant amount of information which can be extracted analytically.

The typical results of numerical solution are shown in Figs. 3 and 4. In Fig. 3 we can see the time evolution of the auxiliary functions $s_1(t)$ to $s_4(t)$. Figure 4 shows the evolution of the switching rate $\lambda(t)$ and average coordinate $\langle \mathsf{X}(t)\rangle$ for nonzero value of the initial condition $\langle \mathsf{Q}_0\rangle$. We can observe qualitatively different behavior for $\epsilon<1$ and $\epsilon>1$: first, the switching rate approaches a nonzero limit for $\epsilon>1$, while for $\epsilon<1$ it decays to zero. This means that in the latter case the system effectively freezes. This is further confirmed by the observation that for $\epsilon<1$ the limit value of the average coordinate depends on the initial conditions, while in the opposite case the dependence on initial conditions is lost for large times, the system equilibrates and the average coordinate converges always to zero. The following sections are mainly devoted to the analytical investigation of the above observations.

### B. Fixed points

The first step in investigating the behavior of the system (22) is the search for the fixed points $[s_3^*, s_4^*]$ of the dynamics.

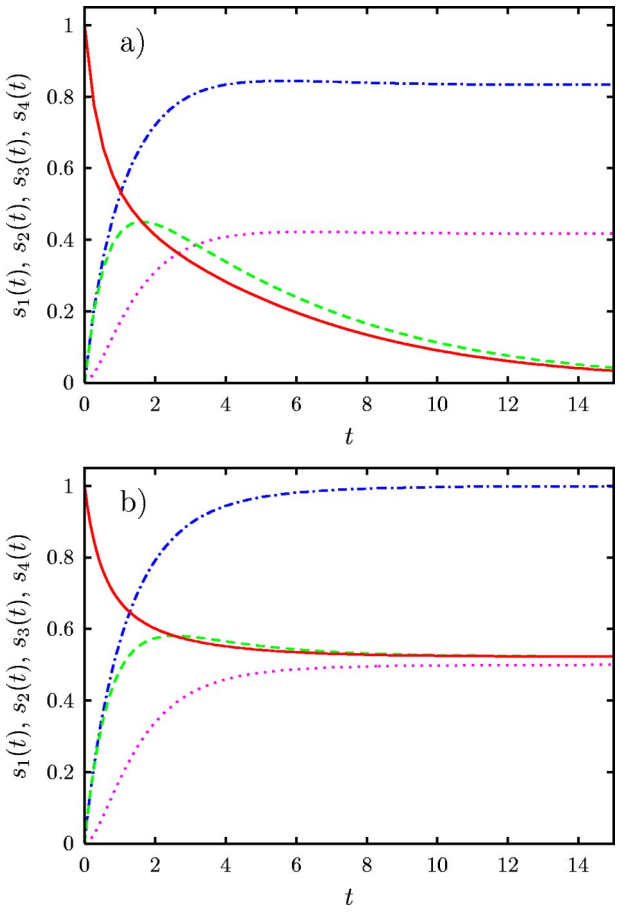


FIG. 3. (Color online) Time evolution of the auxiliary functions $s_1(t)$ (solid line), $s_2(t)$ (dashed line), $s_3(t)$ (dash-dotted line), and $s_4(t)$ (dotted line) for $\gamma-1$ and $q=1$. The panel (a) corresponds to the value of the parameter $\epsilon=1.2$, while in the panel (b) we have $\epsilon=0.8$.

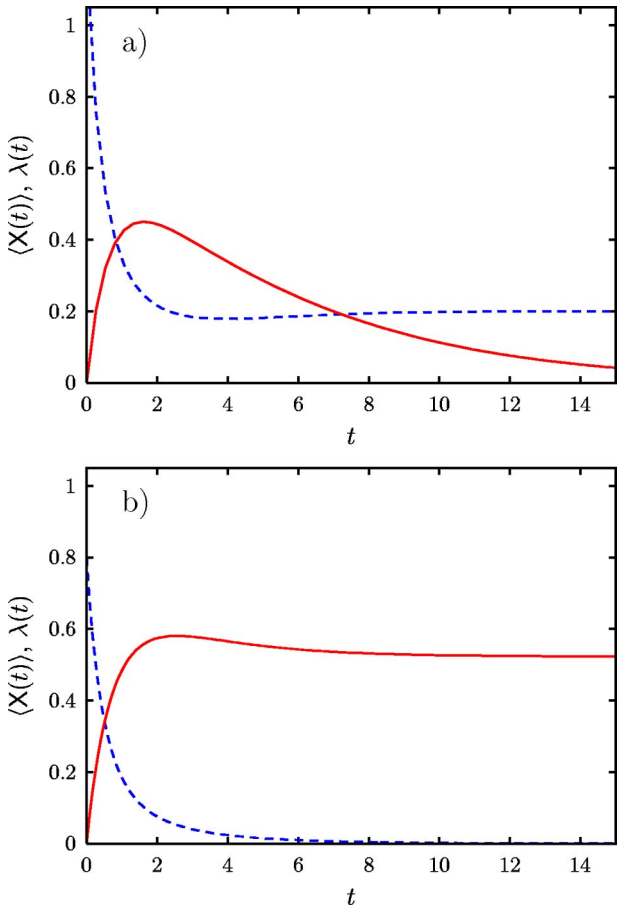


FIG. 4. (Color online) Time evolution of the average coordinate $\langle X(t)\rangle$ computed for initial condition $\langle Q_0\rangle=1$ (solid line) and of the switching rate $\lambda(t)$ (dashed line) for $\gamma=1$ and $q=1$. The panel (a) corresponds to the value of the parameter $\epsilon=1.2$, while in the panel (b) we have $\epsilon=0.8$.

We found that there are only two fixed points, namely,

$$[s_3^*, s_4^*] = \left[\frac{1}{\gamma\epsilon}, \frac{1}{2\gamma^2\epsilon}\right] \tag{23}$$

and

$$[s_3^*, s_4^*] = \left[\frac{1}{\gamma}, \frac{1}{2\gamma^2}\right]. \tag{24}$$

Let us denote $\lambda_\infty$ the value of $\lambda(t)$ calculated at the corresponding fixed point. Using Eq. (21) the fixed point (23) yields $\lambda_\infty=(\epsilon-1)\gamma$ and the fixed point (24) yields $\lambda_\infty=0$.

The linear stability analysis reveals that for $\epsilon>1$ the fixed point (23) is stable, while Eq. (24) is unstable. On the other hand, for $\epsilon<1$ the fixed point (24) is stable, while Eq. (23) is unstable. The case $\epsilon=1$ is a marginal one, where both fixed points have one of the eigenvalues equal to 0. Therefore, the value $\epsilon=1$ marks a transition, whose nature will be further pursued in the following.

### C. Ergodic regime $\epsilon>1$

In this case the relevant fixed point is given in Eq. (23) and inserting its value to the expressions for the moments of $X(t)$ we find that both the average coordinate and the average velocity relaxes to zero. On the other hand, the fluctuations of the coordinate reach positive value, so

$$\lim_{t\to\infty}\langle X(t)\rangle = 0,$$

$$\lim_{t\to\infty}\langle X^2(t)\rangle = \frac{q^2}{\gamma^2\epsilon}. \tag{25}$$

The external force switching rate converges to positive constant $\lim_{t\to\infty}\lambda(t)=\gamma(\epsilon-1)$. In all cases the quantities of interest converge exponentially to their limit values. The rate of convergence is determined by the lowest in absolute value eigenvalue, which is

$$\mu_1 = -\frac{\gamma}{2}(\epsilon - \sqrt{\epsilon^2 - 8\epsilon + 8}). \tag{26}$$

In the interval $\epsilon \in (4-2\sqrt{2}, 4+2\sqrt{2})$ the eigenvalue acquires a nonzero imaginary part, which means that oscillatory behavior is superimposed over the exponential relaxation.

The overall picture is the following. The back-reaction leads to self-adjustment of the switching rate of the external force exerted by the reservoir. The coordinate fluctuates around the origin and these fluctuations are stationary. Therefore, the stationary regime of the system corresponds to the primitive version with fixed $\lambda$, except the fact that the value of $\lambda$ is not given from outside, but tuned by the dynamics itself. We call this regime ergodic, because the particles do not freeze at some value of the coordinate $\mathsf{X}(t)$ but fluctuate forever.

The probability density for the coordinate

$$P(x,t) = \frac{d}{dx}\mathrm{Prob}\{\mathsf{X}(t) \leqslant x\} \tag{27}$$

can be in principle obtained by solving the coupled partial differential equations (analogous to Fokker-Planck equation)

$$\frac{\partial}{\partial t}\begin{pmatrix} p_-(x,t) \\ p_+(x,t) \end{pmatrix} = \frac{\partial}{\partial x}\begin{pmatrix} (\gamma x + q)p_-(x,t) \\ (\gamma x - q)p_+(x,t) \end{pmatrix} - \lambda(t)\begin{pmatrix} 1 & -1 \\ -1 & 1 \end{pmatrix}\begin{pmatrix} p_-(x,t) \\ p_+(x,t) \end{pmatrix}, \tag{28}$$

where $p_\pm(x,t) = (d/dx)\mathrm{Prob}\{\mathsf{X}(t) \leqslant x, \mathsf{Q}(t) = \pm q\}$ and therefore $P(x,t) = p_-(x,t) + p_+(x,t)$. These equations are not analytically solvable, but provide the exact asymptotic probability density. Indeed, for $t \to \infty$ we can set the left-hand side (LHS) of Eq. (28) to zero and the function $\lambda(t)$ on the right-hand side (RHS) to its asymptotic value $\lambda_\infty$. Then, we obtain a set of two ordinary differential equations, which can be solved, giving finally the result [39,46]

$$\lim_{t\to\infty} P(x,t) = \frac{\gamma}{q}\frac{(1-\tilde{x}^2)^{(\epsilon-3)/2}}{B\left(\frac{\epsilon-1}{2}, \frac{1}{2}\right)}\Theta(1-\tilde{x}^2), \tag{29}$$

where $\tilde{x} = x\gamma/q$, $\Theta(a)$ is the Heaviside unit-step function, and $B(a,b)$ denotes the Beta function [47].

We can observe a qualitative change at the value $\epsilon = 3$. For $\epsilon > 3$ the limiting distribution (29) has a maximum for $x = 0$ and approaches 0 at the edges of the support $[-q/\gamma, q/\gamma]$, while for $\epsilon < 3$ it has a minimum at $x = 0$ and diverges at the edges of the support. The tendency for accumulating the probability close to the points $\pm q/\gamma$ when $\epsilon$ decreases can be regarded as a precursory phenomenon of the transition to the nonergodic regime, investigated in the following section.

### D. Nonergodic regime $\epsilon < 1$

In this case we have Eq. (24) as stable fixed point. For $\langle \mathsf{Q}_0 \rangle = 0$ the average coordinate converges to 0 again, but the second moment approaches the $\epsilon$-independent maximum value

$$\lim_{t\to\infty} \langle \mathsf{X}^2(t) \rangle = \frac{q^2}{\gamma^2}. \tag{30}$$

As the probability density for the coordinate $P(x,t)$ has support limited to the interval $[-q/\gamma, q/\gamma]$, it follows from Eq. (30) that the limiting probability density is composed of two $\delta$ functions of equal weight $\frac{1}{2}$ located at the edges of the latter interval. More generally, for nonsymmetric initial condition for the noise, $\langle \mathsf{Q}_0 \rangle \neq 0$, the limiting probability density is the sum of two $\delta$ functions,

$$\lim_{t\to\infty} P(x,t) = \rho_+ \delta\left(x - \frac{q}{\gamma}\right) + \rho_- \delta\left(x + \frac{q}{\gamma}\right), \tag{31}$$

the weights of which depend nontrivially on $\epsilon$ and the initial condition

$$\rho_\pm = \frac{1}{2}\left(1 \pm \frac{\langle \mathsf{Q}_0 \rangle}{q}\sigma(\epsilon)\right), \tag{32}$$

where $\sigma(\epsilon) = \lim_{t\to\infty} s_1(t)$.

The function $\lambda(t)$ relaxes to zero. Therefore, in this regime, the switching of the external force asymptotically stops and the coordinate $\mathsf{X}(t)$ approaches either the value $+q/\gamma$ or $-q/\gamma$, where it freezes. So, the coordinate acquires a random but time-independent asymptotic value. More precisely, the mean coordinate $\langle \mathsf{X}(t) \rangle$ approaches a generally nonzero asymptotic value, which depends on the initial condition. This is the manifestation of glassy state in the regime $\epsilon < 0$, characterized by broken ergodicity and nonzero Edwards-Anderson order parameter. This point will be discussed more in detail later in the presentation of correlation functions.

As in the ergodic phase, all quantities relax toward their limit values exponentially for large times. The rate of convergence is governed by the eigenvalue with smallest modulus, which is now

$$\mu_1 = -2\gamma(1-\epsilon). \tag{33}$$

Note that, contrary to the ergodic regime, the eigenvalue is always a real number, so no oscillations occur, at least in the linearized approximation.

### E. Marginal case $\epsilon = 1$

Let us proceed by approaching the marginal case $\epsilon = 1$ from the nonergodic side, i.e., from below. It might be instructive to cast Eqs. (22) in terms of the eigenmodes of the linearized approximation. Namely, we can introduce the functions

$$\xi(t) = \frac{1}{(2\epsilon-1)\gamma}\left(s_3(t) - \gamma\, s_4(t) - \frac{1}{2\gamma}\right),$$

$$\eta(t) = \frac{1}{(2\epsilon-1)\gamma}\left(-s_3(t) + 2\epsilon\gamma\, s_4(t) + \frac{1-\epsilon}{\gamma}\right), \tag{34}$$

and express Eqs. (22) in the form

$$\dot{\xi} = -2\gamma(1-\epsilon)\xi + 2\epsilon\gamma^3(2\epsilon\,\xi + \eta)\xi,$$

$$\dot{\eta} = -\gamma\ \eta - 2\epsilon\gamma^3(2\epsilon\ \xi + \eta)\xi. \tag{35}$$

The function $\xi(t)$ has a straightforward physical interpretation: it describes the time evolution of the switching rate of the external force. Indeed, inserting Eq. (34) into Eq. (21) we get

$$\lambda(t) = 2\gamma^3(1-2\epsilon)\xi(t). \tag{36}$$

Equations (35) are a convenient starting point for the investigation of the marginal regime. Taking $\epsilon=1$, the linear term in the equation for $\dot{\xi}$ vanishes, while the linear term in the equation for $\dot{\eta}$ remains. This suggests that in the long-time regime the value of $\eta$ will be negligible compared to $\xi$. This consideration will yield the leading term in the relaxation.

Thus, supposing $|\eta| \ll |\xi|$ we get the following approximate equation for $\xi$:

$$\dot{\xi} = 4\gamma^3\ \xi^2, \tag{37}$$

which leads to the following asymptotic behavior

$$\xi(t) \simeq -\frac{1}{4\gamma^3}\frac{1}{t}, \quad t \to \infty. \tag{38}$$

Now we must check the assumption that $\eta$ is negligible compared to $\xi$. However, from Eq. (35) we can see that the leading term in the relaxation of $\eta$ is

$$\eta(t) \simeq \frac{1}{\gamma}\frac{1}{t^2}, \quad t \to \infty, \tag{39}$$

and the assumption is therefore consistent.

The consequence to draw is that in the marginal regime the relaxation becomes power law with exponent −1. Especially, the relaxation of the switching rate follows the behavior

$$\lambda(t) \simeq \frac{1}{2t}, \quad t \to \infty. \tag{40}$$

In Fig. 5 we can compare the numerical solution with the asymptotic behavior (40). We can see not only that the function $\lambda(t)$ approaches zero according to the power decay (40), but also the corrections to the asymptotic behavior can be well approximated by a power. Indeed, from the inset in Fig. 5 we can see that

$$\frac{1}{2t\ \lambda(t)} - 1 \simeq 3\ t^{-0.9}, \quad t \to \infty. \tag{41}$$

It is interesting to note that the power in the correction is not an integer, so the naive expansion of the solution in powers of $t^{-1}$ cannot be used here. Instead, the behavior (41) suggests the expression in the form of a continued fraction

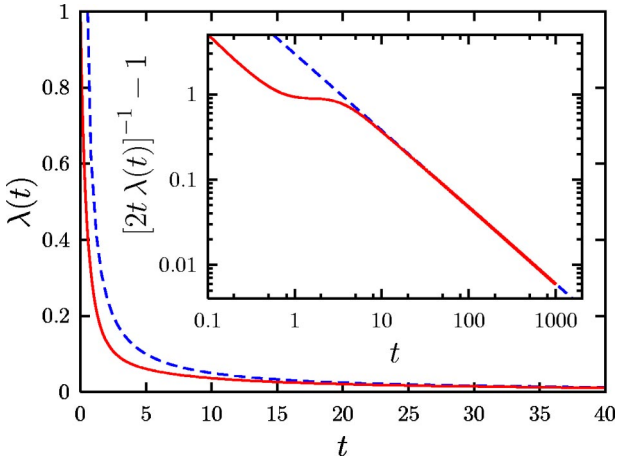


FIG. 5. (Color online) Time evolution of the switching rate in the marginal regime $\epsilon=1$, for $\gamma=1$ and $q=1$. The solid line is the numerical solution, dashed line the asymptotic analytical solution (40). In the inset the deviation from the expression (40) is shown (solid line). The dashed line is power dependence $3\times t^{-0.9}$.

$$\lambda(t) = \cfrac{1}{a_1 t^{\alpha_1} + \cfrac{1}{a_2 t^{\alpha_2} + \cfrac{1}{a_3 t^{\alpha_3} + \cdots}}}, \tag{42}$$

where the values $a_1=2$ and $\alpha_1=1$ are known exactly and the next pair of parameters is estimated from the numerical solution as $a_2 \simeq 1/6$ and $\alpha_2 \simeq 0.9$.

## IV. CORRELATION FUNCTIONS

Additional information on the properties of the transition from ergodic to nonergodic behavior which occurs at the value $\epsilon=1$ can be gained from the two-time correlation functions. Let us have $t > t_1 > 0$ and define the correlation function

$$C(t,t_1) = \langle \mathsf{X}(t)\mathsf{X}(t_1)\rangle. \tag{43}$$

It can be expressed through the functions $s_1(t)$ to $s_4(t)$. The most general formula is

$$\begin{aligned} C(t,t_1) = {} & \langle \mathsf{X}_0\rangle e^{-\gamma(t+t_1)} + \langle \mathsf{X}_0\mathsf{Q}_0\rangle[e^{-\gamma t_1}\ s_2(t) + e^{-\gamma t}\ s_2(t_1)] \\ & + q^2\Big[2e^{-\gamma(t-t_1)}\ s_4(t_1) + [s_2(t) \\ & - e^{-\gamma(t-t_1)}\ s_2(t_1)]\frac{s_3(t_1)}{s_1(t_1)}\Big], \end{aligned} \tag{44}$$

although we suppose throughout this section that $\mathsf{X}_0=0$.

We show in Figs. 6 (ergodic regime) and 7 (nonergodic regime) the evolution of correlation functions using the numerical solution for $s_1$ to $s_4$. We can observe the damping of the correlations in the ergodic regime, while in the nonergodic regime the correlations converge to a finite limit. Let us now turn to the analytic investigation of the long-time behavior of the correlation function.

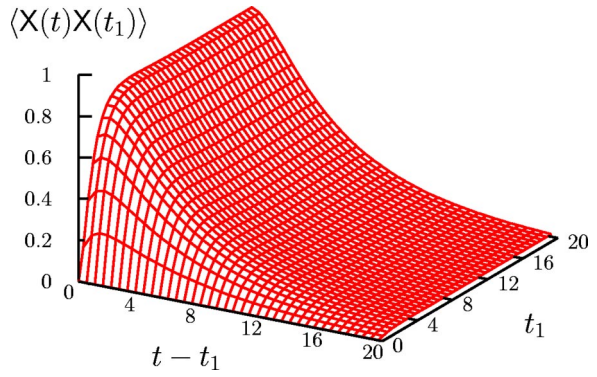


FIG. 6. (Color online) Correlation function in the ergodic regime, for $\epsilon=1.2$, $\gamma=1$ and $q=1$.

For long enough times we can suppose that we are in the regime of exponential asymptotic relaxation of the functions $s_1(t)$ to $s_4(t)$ and $\lambda(t)$, which is governed by the eigenvalue closest to 0, as given by Eqs. (26) and (33).

Let us start with the ergodic regime $\epsilon>1$. We find that for both $t\to\infty$ and $t_1\to\infty$ the correlation function behaves like

$$C(t,t_1) \simeq \frac{q^2}{\gamma^2\epsilon(2-\epsilon)}[e^{-\gamma(\epsilon-1)(t-t_1)} - (\epsilon-1)e^{-\gamma(t-t_1)}]. \tag{45}$$

Important feature of this result is that the correlation in asymptotic regime depends only on the time difference $t-t_1$ and decays to zero when this difference increases. This supports the picture of the $\epsilon>1$ phase as a usual ergodic regime without long-time correlations.

The situation is dramatically different for $\epsilon<1$. Technically speaking, it is important that the function $\Lambda(t)$ has a finite limit for large times, $\lim_{t\to\infty}\Lambda(t)=\Lambda_\infty<\infty$. For $\epsilon$ close to 1 (i.e., $1-\epsilon\ll 1$) the approach to this limit value can be written in the form

$$\Lambda(t) \simeq \Lambda_\infty - \theta\, e^{-2\gamma(1-\epsilon)t}, \tag{46}$$

where $\theta$ is a constant depending on $\epsilon$.

For large times the correction will be small and we can formally write the correlation function as expansion in powers of $\theta$. However, we should bear in mind that it is not $\theta$ itself, which is small, but the factor $e^{-2\gamma(1-\epsilon)t}$ which appears always together with $\theta$.

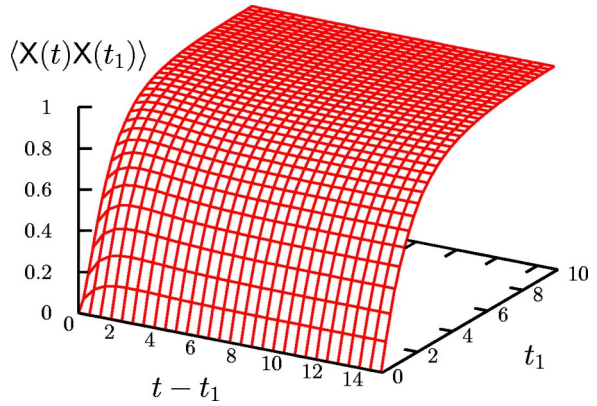


FIG. 7. (Color online) Correlation function in the nonergodic regime, for $\epsilon=0.8$, $\gamma=1$ and $q=1$.

Finally,

$$C(t,t_1) \simeq \frac{q^2}{\gamma^2} + \frac{\theta q^2}{(\gamma-\mu)\gamma}(e^{-\mu\, t} - e^{-\mu\, t_1}) - \frac{2\theta q^2\mu}{(\gamma-\mu)(2\gamma-\mu)\gamma}e^{-\gamma(t-t_1)-\mu\, t_1} + O(\theta^2), \tag{47}$$

using $\mu=2\gamma(1-\epsilon)$ for shorter notation.

We can see that the qualitative difference from the ergodic regime consists in the fact that for $\epsilon<1$ the correlation function converges to a positive $\epsilon$-independent constant $q^2/\gamma^2$. If we define the Edwards-Anderson order parameter

$$q_{\mathrm{EA}} = \lim_{\tau\to\infty}\lim_{t_1\to\infty} C(t_1+\tau,t_1), \tag{48}$$

we can see that $q_{\mathrm{EA}}$ jumps discontinuously from the value $q_{\mathrm{EA}}=0$ for $\epsilon>1$ to $q_{\mathrm{EA}}=q^2/\gamma^2$ for $\epsilon<1$. This observation represents another evidence that there is a transition from ergodic regime to nonergodic glassy regime at $\epsilon=1$. As the Edwards-Anderson parameter is discontinuous at the critical point, the transition should be classified as first order from this point of view. However, because we do not deal with an equilibrium transition and the phenomenon is of purely dynamical origin, the canonic classification of phase transition as first or second order is of limited relevance here.

## V. CRITICAL BEHAVIOR AT $\epsilon\to 1^-$

We have already seen that it is possible to characterize the glass transition at $\epsilon=1$ through the Edwards-Anderson order parameter $q_{\mathrm{EA}}$. It has discontinuity at the transition, so the corresponding critical exponent is 0. Here we investigate another quantity, which can play the role of an order parameter, being zero in the ergodic and nonzero in the nonergodic phase.

The quantity in question will describe how the initial conditions affect the asymptotic value of the average coordinate. We have already touched this point in Sec. III D. Up to now we assumed that the initial condition for the noise is such that $\langle Q_0\rangle=0$. This assumption has the consequence that both in ergodic and nonergodic regimes the average coordinate converges to 0. In this section we investigate the case $\langle Q_0\rangle \neq 0$.

From Eqs. (15) and (18) we can see that

$$\lim_{t\to\infty}\langle X(t)\rangle = \frac{\langle Q_0\rangle}{\gamma}\sigma(\epsilon), \tag{49}$$

where we defined, as in Sec. III D,

$$\sigma(\epsilon) = \lim_{t\to\infty} s_1(t), \tag{50}$$

stressing explicitly the dependence on $\epsilon$. Equations (22) hold also in case $\langle Q_0\rangle\neq 0$. Therefore, we can proceed without

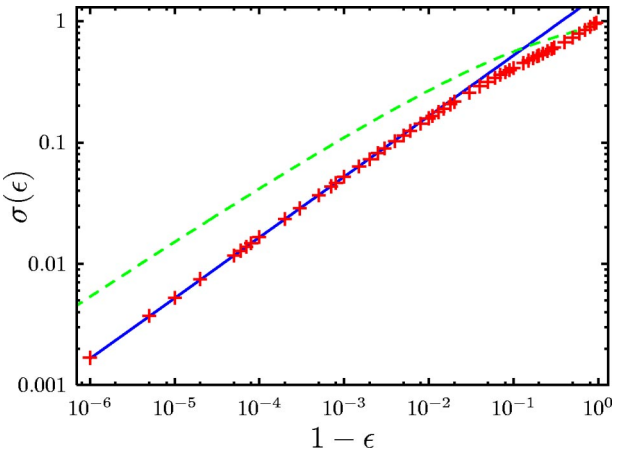


FIG. 8. (Color online) The critical behavior at $\epsilon \to 1$. Points (+) are results of numerical integration. The solid line is the approximation (56), while the dashed line is the exact upper bound $\sigma_{\mathrm{upper}}(\epsilon)$ given by formula (55).

further complications. We only need to plug the solution obtained the same way as in Secs. III and IV into the definition (11) of the function $s_1(t)$ and find the limit (50).

Let us first present the results of numerical integration. We will turn to the analytic estimate afterwards. Figure 8 shows the results of numerical integration, indicating that asymptotically for $\epsilon \to 1$ the behavior follows the power law

$$\sigma(\epsilon) \sim (1-\epsilon)^{1/2}. \tag{51}$$

The exponent $1/2$ is still observed only empirically and we do not possess any proof that this is the exact value.

However, we may get some analytical argument in favor of this type of behavior from Eqs. (19)–(21), which can be rewritten in slightly different form. Defining new function $\psi(t)=s_3(t)-1/\gamma$ we can write the set of equations for the pair $\psi(t)$ and $\lambda(t)$,

$$\dot{\psi} = -\gamma\,\psi - \frac{1}{\gamma}\lambda - \lambda\psi,$$

$$\dot{\lambda} = -2\gamma(1-\epsilon)\lambda + 2\epsilon\gamma^2\,\lambda\psi, \tag{52}$$

with initial conditions $\psi(0)=-1/\gamma$, $\lambda(0)=\epsilon\gamma$. If we further define $\Lambda_\infty=\int_0^\infty \lambda(t)dt$ and $\Psi_\infty=\int_0^\infty \psi(t)dt$, we can integrate both LHS and RHS of Eqs. (52) and obtain the exact relation between $\Lambda_\infty$ and $\Psi_\infty$,

$$\epsilon = -2\Lambda_\infty - 2\epsilon\gamma^2\,\Psi_\infty. \tag{53}$$

Knowing $\Lambda_\infty$ would solve the problem, because $\sigma(\epsilon)=e^{-\Lambda_\infty}$. However, in addition to Eq. (53) we need some other condition. It can be established from the observation that the equation for $\lambda(t)$ can be formally solved in the form

$$\lambda(t) = \epsilon\gamma \exp\left(-2\gamma(1-\epsilon)t + 2\epsilon\gamma^2\int_0^t \psi(t')dt'\right), \tag{54}$$

and because $\psi(t)<0$, we have $\int_0^t \psi(t')dt' > \Psi_\infty$. Therefore, we can write the following upper bound:

$$\sigma(\epsilon) < \exp\left[-\frac{1}{2}W_{\mathrm{L}}\left(\frac{\epsilon\, e^{-\epsilon}}{1-\epsilon}\right)\right] \equiv \sigma_{\mathrm{upper}}(\epsilon), \tag{55}$$

where $W_{\mathrm{L}}(x)$ is the Lambert function defined by the equation $W_{\mathrm{L}}(x)e^{W_{\mathrm{L}}(x)}=x$.

The leading term in the asymptotic behavior of the Lambert function for large argument is $W_{\mathrm{L}}(x)\simeq \ln x$. If we use it as an approximation for calculating the asymptotic behavior of $\sigma(\epsilon)$, starting with Eq. (55) we finally get

$$\sigma(\epsilon) \simeq \sqrt{e}\,\sqrt{1-\epsilon}, \tag{56}$$

which is compatible with the behavior (51). Actually, we can see in Fig. 8 that the approximation (56) fits very well with the results from numerical integration and lies much closer than the exact upper bound (55). Thus, we conjecture that the formula (56) is in fact the correct asymptotic behavior for $\epsilon \to 1$.

To sum up, in the regime $\epsilon > 1$, the initial conditions are irrelevant for long-time dynamics, as expected in the ergodic phase. On the other hand, for $\epsilon < 1$, we observe that the asymptotic value of the average coordinate depends on the initial condition for the noise, which is yet another signature of ergodicity breaking. The factor $\sigma(\epsilon)$ measures the sensitivity to initial conditions: it vanishes in ergodic phase but remains nonzero in nonergodic phase. So, it may be considered as a kind of order parameter. Close to the critical point $\epsilon=1$ it approaches zero continuously as a power with critical exponent $1/2$.

## VI. RESPONSE TO HARMONIC PERTURBATION

Let us investigate now the response of the particle to the external driving force. Adding the additional term $F(t)=F_0\cos(\omega t)$ at the right-hand side of Eq. (1), one can repeat, *mutatis mutandis*, all steps leading to the system of equations for the functions $s_1(t)$ to $s_4(t)$. We find that Eqs. (17)–(20) hold unchanged, while the influence of the external force modifies the expression (21) for $\lambda(t)$. Actually, in the present case one gets

$$\frac{\lambda(t)}{\epsilon\gamma} = 1 - 2\gamma\, s_3(t) + 2\gamma^2\, s_4(t) + \frac{1}{q^2}\left(\gamma\, e^{-\gamma t}\int_0^t F(t')e^{\gamma t'}\,dt' - F(t)\right)^2. \tag{57}$$

We assumed $\langle \mathrm{Q}_0\rangle = 0$ and $\langle \mathrm{X}_0\rangle = 0$ here.

First quantity to study is the response of the average coordinate. We find

$$\langle \mathrm{X}(t)\rangle = \langle \mathrm{Q}_0\rangle\, e^{-\gamma t}\int_0^t e^{-\Lambda(t')+\gamma t'}\,dt' + e^{-\gamma t}\int_0^t F(t')e^{\gamma t'}\,dt'. \tag{58}$$

Obviously enough, in the stationary regime the average coordinate oscillates around 0 with the same frequency as the driving force $F(t)$. We arrive at the standard Debye-type dynamic susceptibility

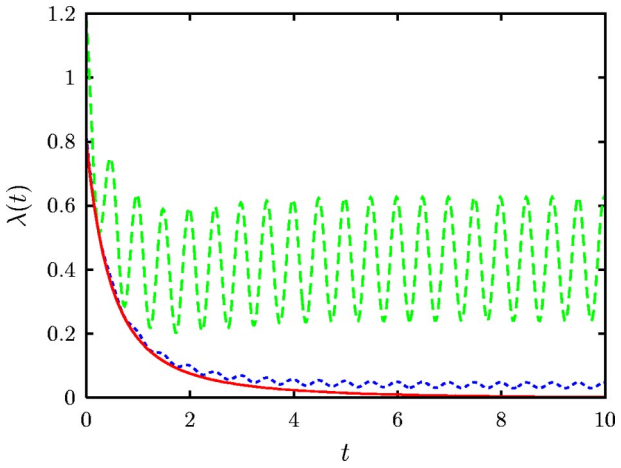


FIG. 9. (Color online) Response of the switching rate to harmonic external driving force for $\gamma=1$, $q=1$, $\epsilon=0.8$, $\omega=2\pi$, and $F_0=0.7$ (dashed line) and $F_0=0.15$ (dotted line). The solid line shows the time dependence in the absence of the external driving force.

$$\chi(t-t') = \Theta(t-t')e^{-\gamma(t-t')}. \tag{59}$$

Thus, the exact response in terms of the coordinate is linear. This behavior also does not depend on the value of $\epsilon$.

The situation becomes much more complicated when we turn to quantities, which depend nonlinearly on the coordinate, especially the switching rate $\lambda(t)$. We solved numerically the set of equations (17)–(20) and (57). We can see in Fig. 9 the evolution of the function $\lambda(t)$ within the nonergodic regime, with $\epsilon=0.8$. Comparing the behavior with the evolution in the absence of the external harmonic perturbation we can see that the switching rate $\lambda(t)$ does not approach zero any more, but it oscillates around some finite value, which we will denote by $A_0$. This qualitative feature holds for whatever small external force. However, when the amplitude $F_0$ of the external field goes to zero, also the value of $A_0$ approaches zero according to $A_0 \sim {F_0}^2$, as can be seen from Fig. 10. Generalizing the linear stability analysis of Sec. III B to harmonic oscillations, we conclude that the external field continuously shifts the fixed point, with $\lambda=0$ (i.e., also $A_0=0$), to a position with positive $A_0$, but the value of the shift vanishes when the amplitude of the perturbation goes to zero.

Figure 11 exemplifies the evolution of the functions $s_3(t)$ and $s_4(t)$. We can clearly see that the oscillations are not harmonic. Generally, in the stationary regime these functions are nonharmonic but periodic with the doubled frequency $2\omega$. Thus, the same holds also for the function $\lambda(t)$. Using Eq. (57) the stationary response in terms of the switching rate can be written as Fourier series

$$\lambda_{\mathrm{st}}(t) = A_0 + \sum_{k=1}^{\infty} (A_k \sin 2k\omega t + B_k \cos 2k\omega t). \tag{60}$$

The amplitudes of the harmonic components $A_0$, $A_k$, $B_k$, $k=1,2,\ldots$, satisfy a complicated infinite set of quadratic equations.

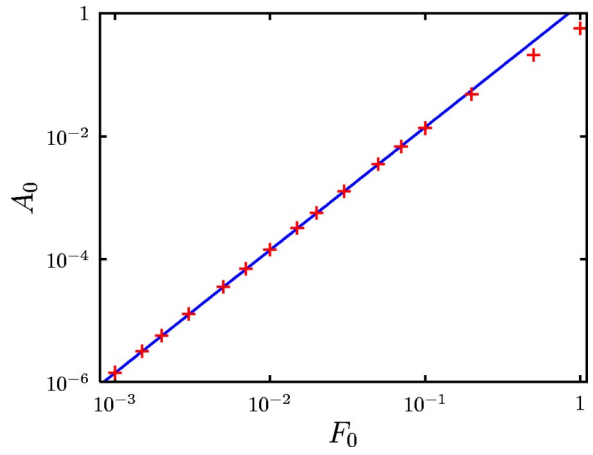


FIG. 10. (Color online) Dependence of the constant term in the Fourier series (60) for $\lambda_{\mathrm{st}}(t)$ on the amplitude of the driving force (+), in the regime $\epsilon<1$. The parameters are $\gamma=1$, $q=1$, $\epsilon=0.8$, and the frequency is $\omega=\pi/2$. Full line is the function $1.4F_0^2$.

To assess the weight of the higher harmonics we performed the fast Fourier transform of the time evolutions obtained by numerical solution, throwing away the initial transient regime. To illustrate the presence of higher harmonics we chose the function $s_3(t)$. The modulus of its Fourier transform $\hat{s}_3(\nu)=\int s_3(t)e^{-2\pi i\ \nu t}\ dt$ is shown in Fig. 12. We can clearly see the peaks at the multiples of the basic frequency. We can also observe that the higher harmonics have quite considerable weight. In the inset of Fig. 12 we show also the Fourier transform of the function $\lambda(t)$. Here, the higher harmonics are much less pronounced.

The most important feature of the time evolution under the influence of external harmonic force is the observation that the switching rate remains always positive. This leads to the already mentioned fact that whatever is the coupling strength parameter $\epsilon$, the mean coordinate in stationary regime oscillates around zero, irrespective of the initial conditions. However, this is the signature of ergodicity, so the glassy behavior disappears under the influence of arbitrarily small external perturbation. Such a behavior was already ob-

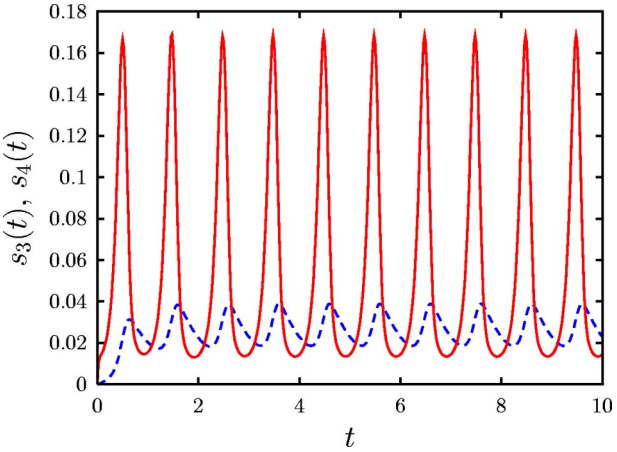


FIG. 11. (Color online) Response of the functions $s_3(t)$ (solid line) and $s_4(t)$ (dashed line) to harmonic external driving force for $\gamma=1$, $q=1$, $\epsilon=0.8$, $\omega=\pi$, and $F_0=10$.

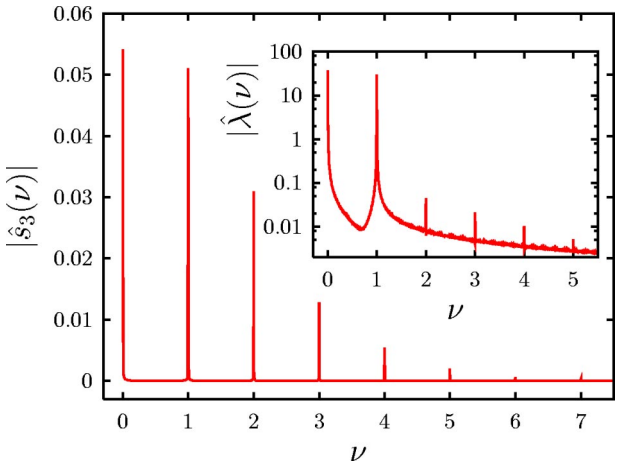


FIG. 12. (Color online) Fourier transform of the stationary oscillations of the function $s_3(t)$ under the influence of harmonic external driving force for $\epsilon=0.8$, $\omega=\pi$, and $F_0=10$. It was calculated using the fast Fourier transform algorithm. In the inset the Fourier transform of oscillations of the switching rate. The finite width of the peaks, the noise, and the continuous part of the spectrum in the inset are due to numerical imprecision of the fast Fourier transform procedure.

served also in the model of sheared colloid [25].

Both observations can be easily understood. The external force drags the particle back and forth. Once moving, the particle induces through the back-reaction (2) the fluctuations of the environmental force, which prevents the system from freezing in a nonergodic state. This holds for any positive amplitude of the driving force. However, when the force diminishes, there is still longer transient period, where the system apparently relaxes toward the arrested state, as can be seen qualitatively in Fig. 9. In the limit of infinitesimally small driving, the transient time blows up and the asymptotic state corresponds to the dynamically arrested state. This picture is consistent with the view of glassiness as a purely dynamical phenomenon.

We also observed the response of the system to a signal, which is switched on only after the system relaxed very close to the arrested state. The results can be seen in Fig. 13. Initially, the switching rate relaxes toward zero, but after the perturbation it settles on oscillating behavior. The average coordinate initially approaches nonzero value (we have chosen initial condition $\langle Q_0\rangle>0$), but the perturbation brings it to oscillations around zero. This can be interpreted as a schematic picture of shear thinning, although the model is too much simplified to account for the shear thinning quantitatively.

We also looked at the role of fluctuation-dissipation theorem (FDT) in our model. Usually in ergodic systems in equilibrium it relates the correlation and response functions through the identity $\partial C(t,t')/\partial t' = T\,\chi(t,t')$. Comparing Eqs. (45) and (59) we can see that strictly speaking FDT is not satisfied. However, a more general formula of the form

$$\frac{\partial}{\partial t'}C(t,t') = \frac{q^2(\epsilon-1)}{\gamma\epsilon(\epsilon-2)}[\chi(t,t') - \chi^{\epsilon-1}(t,t')] \qquad (61)$$

holds here. Thus, the quantity $[q^2(\epsilon-1)/\gamma\epsilon(\epsilon-2)](1-\chi^{\epsilon-2})$ plays the role of a (generalized, time-dependent) temperature. This is consistent with the interpretation, given in Sec. II A, of $\gamma$ as a parameter proportional to inverse temperature. However, we should keep in mind that the influence of parameters $\gamma$ and $\epsilon$ is mixed in Eq. (61).

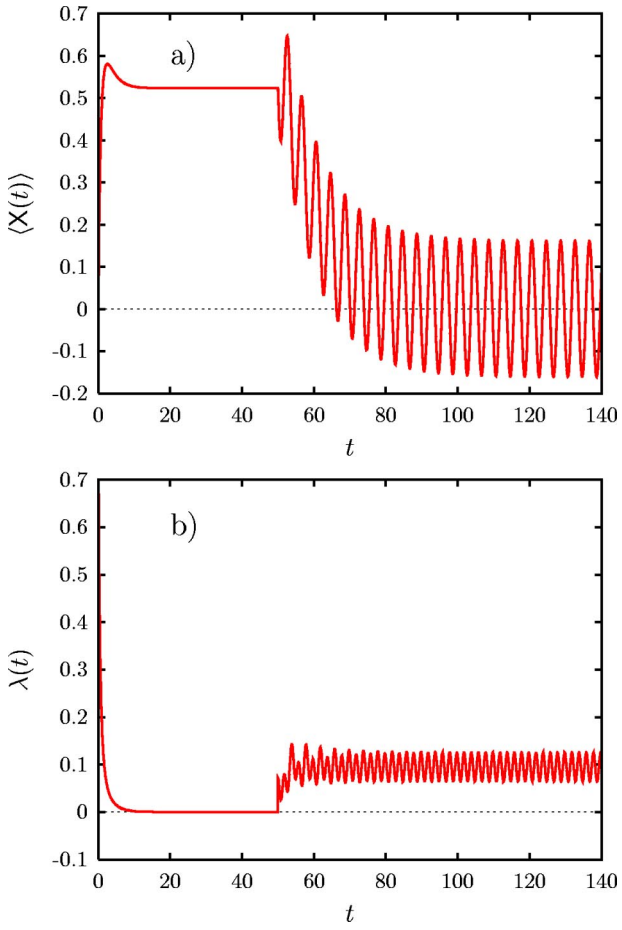


FIG. 13. (Color online) Time evolution of the average coordinate (a) and switching rate (b) in the regime $\epsilon<1$, when the external harmonic perturbation was switched on at time $t=50$. The parameters are $\gamma=1$, $q=1$, $\epsilon=0.8$, the amplitude of the external perturbation is $F_0=0.3$, and the frequency is $\omega=\pi/2$. The initial condition is $\langle Q_0\rangle=1$.

As for the nonergodic regime, FDT is not expected to be valid. Indeed, we found that neither standard FDT nor a generalized form of the type (61) or those found in aging systems [36] applies here. Generalized FDT in the form studied in Ref. [36] implies a "weak" ergodicity breaking. From this point of view we have a "strong" ergodicity breaking in our model.

## VII. CONCLUSIONS

Motivated by the dynamical arrest phenomenon in colloids, we formulated and solved a stochastic dynamical model, where the coordinate of a single particle evolves under the influence of stochastic environmental force. The back-reaction couples the switching rate of the force to the average of the square of the velocity of the particle. The strength of the coupling $\epsilon$ is the crucial parameter which

determines the behavior of the system. The problem reduces to a set of coupled nonlinear differential equations, which was investigated both analytically and numerically.

The back-reaction induces a phase transition from the ergodic phase for $\epsilon > 1$ to the nonergodic glassy state for $\epsilon < 1$. The transition is observed qualitatively in the behavior of the switching rate, decaying to zero in nonergodic state, while staying positive in the ergodic state. The Edwards-Anderson parameter, established from the two-time correlation functions, is discontinuous at the transition; it is zero in ergodic phase ($\epsilon > 1$), while for $\epsilon < 1$ it acquires finite value independent of $\epsilon$. The critical point $\epsilon = 1$ is characterized by power-law decay of the switching rate. The leading term $\sim t^{-1}$ in the long-time behavior was calculated analytically.

We investigated the critical behavior at $\epsilon \to 1$ through the dependence of the average coordinate in the long-time limit on the initial condition. We find that the asymptotic value of the average coordinate is proportional to the average initial value of the force, where the proportionality factor $\sigma(\epsilon)$ is singular at the transition. In the ergodic phase we have $\sigma(\epsilon) = 0$ identically, while in the nonergodic phase, close to the transition, we found $\sigma(\epsilon) \sim (1-\epsilon)^{1/2}$ for $\epsilon \to 1^-$.

Therefore, we find a situation quite unusual from the point of view of static equilibrium phase transition. Indeed, we have two variables, which may be considered as order parameter, namely, the Edwards-Anderson parameter and the quantity $\sigma(\epsilon)$. While the former is discontinuous at the critical point, thus indicating first-order transition, the latter is continuous, suggesting second-order transition. The discrepancy is to be attributed to purely dynamical nature of the transition.

Finally, we investigated the response of the system to harmonic external perturbation. We found that the exact response of the coordinate is linear. On the other hand, the response of the variables which are quadratic functions of the coordinate and velocity, such as the switching rate, was nonlinear and generically contains all higher harmonics, as was seen in the Fourier transform of the signal. We also observed that arbitrarily weak external perturbation is sufficient to "melt" the nonergodic glassy state and bring it back to ergodic behavior. We may relate this feature to the notion of stochastic stability [48]; in this view our system is not stochastically stable. However, our finding is in accord with previously observed behavior of sheared colloids [25]. It makes also connection to the rheological properties of thixotropic fluids [49,50], although our model is too simplified to give quantitative predictions in this direction.

The back-reaction mechanism described by Eq. (2) represents the simplest choice. One may ask what would happen if we tried another prescription. We expect that the methods used here will be as well applicable if we generalize Eq. (2) as $\lambda(t) = \langle F(\mathsf{V}^2(t)) \rangle$ for an analytic function $F(x)$. More complicated situation would appear if the dependence was nonlocal in time, e.g., of the form $\lambda(t) = \int^t \langle \mathsf{V}(t)\mathsf{V}(t') \rangle \, K(t-t')dt'$ with some kernel $K(t)$. Such an approach would bring our model closer to the well-studied mode coupling equations, but it goes beyond the scope of the present work.

## ACKNOWLEDGMENTS

This work was supported by Project No. 202/03/0551 of the Grant Agency of the Czech Republic.

[1] C. A. Angell, Science **267**, 1924 (1995).
[2] R. G. Palmer, D. L. Stein, E. Abrahams, and P. W. Anderson, Phys. Rev. Lett. **53**, 958 (1984).
[3] G. Paladin, M. Mézard, and C. de Dominicis, J. Phys. (France) Lett. **46**, L-985 (1985).
[4] T. R. Kirkpatrick and D. Thirumalai, Phys. Rev. Lett. **58**, 2091 (1987).
[5] T. R. Kirkpatrick and D. Thirumalai, Phys. Rev. B **36**, 5388 (1987).
[6] T. R. Kirkpatrick, D. Thirumalai, and P. G. Wolynes, Phys. Rev. A **40**, 1045 (1989).
[7] F. Ritort, Phys. Rev. Lett. **75**, 1190 (1995).
[8] S. Franz and J. Hertz, Phys. Rev. Lett. **74**, 2114 (1995).
[9] L. F. Cugliandolo and J. Kurchan, Phys. Rev. Lett. **71**, 173 (1993).
[10] S. Franz, M. Mézard, G. Parisi, and L. Peliti, Phys. Rev. Lett. **81**, 1758 (1998).
[11] A. Barrat, R. Burioni, and M. Mézard, J. Phys. A **29**, 1311 (1996).
[12] J. Kurchan, J. Phys. I **2**, 1333 (1992).
[13] L. F. Cugliandolo and J. Kurchan, Philos. Mag. B **71**, 501 (1995).
[14] E. Marinari, G. Parisi, and F. Ritort, J. Phys. A **27**, 7647 (1994).
[15] T. M. Nieuwenhuizen, J. Phys. A **31**, L201 (1998).
[16] A. Cavagna, I. Giardina, and G. Parisi, Phys. Rev. Lett. **83**, 108 (1999).
[17] A. Cavagna, I. Giardina, and G. Parisi, J. Phys.: Condens. Matter **12**, 6295 (2000).
[18] M. Mézard and G. Parisi, Phys. Rev. Lett. **82**, 747 (1999).
[19] B. Coluzzi, G. Parisi, and P. Vervocchio, Phys. Rev. Lett. **84**, 306 (2000).
[20] L. F. Cugliandolo, J. Kurchan, G. Parisi, and F. Ritort, Phys. Rev. Lett. **74**, 1012 (1995).
[21] G. Parisi and F. Slanina, Phys. Rev. E **62**, 6554 (2000).
[22] K. Kawasaki and B. Kim, Phys. Rev. Lett. **86**, 3582 (2001).
[23] S. M. Fielding, P. Sollich, and M. E. Cates, J. Rheol. **44**, 323 (2000).
[24] M. Fuchs and M. E. Cates, Faraday Discuss. **123**, 267 (2003).
[25] M. E. Cates, e-print cond-mat/0211066.
[26] A. M. Puertas, M. Fuchs, and M. E. Cates, Phys. Rev. Lett. **88**, 098301 (2002).
[27] M. Fuchs and M. E. Cates, Phys. Rev. Lett. **89**, 248304 (2002).
[28] E. Zaccarelli, G. Foffi, K. A. Dawson, S. V. Buldyrev, F. Sciortino, and P. Tartaglia, Phys. Rev. E **66**, 041402 (2002).
[29] A. Lawlor, D. Reagan, G. D. McCullagh, P. De Gregorio, P. Tartaglia, and K. A. Dawson, Phys. Rev. Lett. **89**, 245503 (2002).
[30] E. Stiakakis, D. Vlassopoulos, B. Loppinet, J. Roovers, and G.

Meier, Phys. Rev. E **66**, 051804 (2002).
[31] L. Fabbian, W. Götze, F. Sciortino, P. Tartaglia, and F. Thiery, Phys. Rev. E **59**, R1347 (1999).
[32] M. E. Cates, J. P. Wittmer, J.-P. Bouchaud, and P. Claudin, Physica A **263**, 354 (1999).
[33] E. Bertrand, J. Bibette, and V. Schmitt, Phys. Rev. E **66**, 060401 (2002).
[34] W. Götze, in *Liquids, Freezing and Glass Transition*, edited by J. P. Hansen, D. Levesque, and J. Zinn-Justin (North-Holland, Amsterdam, 1991), p. 287.
[35] W. Götze and L. Sjögren, Rep. Prog. Phys. **55**, 241 (1992).
[36] J. P. Bouchaud, L. F. Cugliandolo, J. Kurchan, and M. Mézard, in *Spin Glasses and Random Fields*, edited by A. P. Young (World Scientific, Singapore, 1997), p. 161.
[37] L. Sjögren, Physica A **322**, 81 (2003).
[38] L. Cugliandolo and J. Kurchan, Physica A **263**, 242 (1999).
[39] P. Chvosta and F. Slanina, J. Phys. A **35**, L277 (2002).
[40] W. Horsthemke and R. Lefever, *Noise-Induced Transitions. Theory and Applications in Physics, Chemistry and Biology*, Springer Series in Synergetics Vol. 15 (Springer, Berlin, 1984).
[41] D. R. Cox, *Renewal Theory* (Wiley, New York, 1962).
[42] D. L. Snyder, *Random Point Processes* (Wiley, New York, 1975).
[43] S. Ciliberti, T. S. Grigera, V. Martin- Mayor, G. Parisi, and P. Verrocchio, e-print cond-mat/0312073.
[44] Y. Pomeau, J. Stat. Phys. **24**, 189 (1981).
[45] P. Sibani and N. G. van Kampen, Physica A **122**, 397 (1983).
[46] A. Morita, Phys. Rev. A **41**, 754 (1990).
[47] *Handbook of Mathematical Functions*, edited by M. Abramowitz and I. A. Stegun (Dover, New York, 1970).
[48] G. Parisi, in *Disordered and Complex Systems*, edited by Peter Sollich, A. C. C. Coolen, L. P. Hughston, and R. F. Streater, AIP Conf. Proc. No. 553 (AIP, Melville NY, 2001), e-print cond-mat/0007347.
[49] C. Völtz, M. Nitschke, L. Heymann, and I. Rehberg, Phys. Rev. E **65**, 051402 (2002).
[50] P. Coussot, Q. D. Nguyen, H. T. Huynh, and D. Bonn, Phys. Rev. Lett. **88**, 175501 (2002).